

Matlab Simulation of Photovoltaic System for Speed Control of BLDC Motor

Poonam Lodhi, Hitesh Joshi, Pankaj Kumar

Abstract— In this paper we have carried out the speed control of the brush-less direct current (BLDC) motor and studied the behavior of the motor by analyzing performance parameters, being modeled and simulated in the MATLAB 2011b. The BLDC motor is now used in various industrial and medical applications due to their simple construction, high efficiency, good dynamic response and reliability. The motor is operated using the photovoltaic (PV) array, which is having the input of constant solar irradiation. The maximum power through which the PV array is made to operate for highest efficiency is tracked using the maximum power point tracking (MPPT) method. The MPPT method is developed using perturb and observe (P & O) algorithm. The dc-dc buck converter is employed for the stepping-up of the voltage as per the requirement. The signals in the pulse-width modulation (PWM) generator is developed using the PI controller, Phase-locked loop (PLL), Park's and Clarke's methods.

Keywords- BLDC, MPPT, PV array, P & O, PI controller, PLL, PWM.

1 INTRODUCTION

The energy requirements of the world today are fulfilled by various types of energy sources. The conventional energy sources, i.e. coal, oil and natural gas is mainly used to satisfy this demand, and accounts for almost four-fifth of the total share, and this scenario remains unchanged from over a past decade. These fossil fuels continue to remain dominant sources of energy, primarily because they are relatively inexpensive and currently abundant, are energy rich, and the global infrastructure today is well positioned to produce, deliver and use them. Nonetheless, given the emerging scenario, it is of utmost importance to explore and understand the various other viable alternatives to conventional energy. A country like India, with has a such large population of over one billion and rapid economic growth rate, no single energy resource or technology can act as a panacea to address all issues related to availability of fuel supplies.

Utilization, Suresh Gyan Vihar University, Jaipur, PH-9896998967. E-mail: rudrraa777@gmail.com

Therefore, it is necessary that all non-carbon emitting resources become an integral part of an energy mix, as diversified as possible to ensure energy security to a country like India. Although renewable energy technologies currently represent a fraction of the energy market in India, they have tremendous potential to undergo rapid growth and provide alternative solution to fossil fuels. With varied agro climatic zones providing sufficient raw sources like sunlight, wind, flowing water and flora, India offers ample opportunities to shift to large scale use of new renewable energy sources. The increase in production of renewable energy, inter alia, entails an active involvement of business and financial institutions backed by adequate support and an enabling policy environment from the Government. Given the strong support provided by the Government, India has the potential to position itself as a world leader in the drive to leverage the expertise and resources of businesses and private investors. With such strong support from the Government, backed by concrete measures, renewable energy is likely to become the cornerstone of energy sector, with focus on clean energy, which would have enormous potential.

This paper deals with the basic ideology developed for the use of one kind of renewable source of energy which is

- **Poonam Lodhi** is currently pursuing masters degree program in electrical power systems in Suresh Gyan Vihar University, Jaipur, PH-8302214291. E-mail: lodhi.poonam18@gmail.com
- **Hitesh Joshi** is currently pursuing masters degree program in electrical power systems in Suresh Gyan Vihar University, Jaipur, PH-90241588398. E-mail: haitijoshi@gmail.com
- Pankaj Kumar is currently working at as Asstt. Professor & Scientist at Centre of Excellence, Solar Energy Research &

abundantly found in the country and is considered as a main alternative which can meet all the power needs of the country, which is today suffering the consequences of the unavailability and harmful nature of the fossil fuels. The solar energy is used to construct a PV array, which is using several solar cells connected in series and parallel combinations. The PV array is used for driving the brushless direct current (BLDC) motor load. The BLDC motor which is here used is gaining special attention among the industrial consumers due to various advantages of the motor.

2 Solar Cell Modeling

A solar cell is considered to be the basic building block for a solar panel. A photovoltaic module can be formed by taking the series and parallel combinations of the solar cells and connecting them accordingly. Solar cell is basically a p-n junction fabricated in a thin wafer or layer of semiconductor. The electromagnetic radiation of the solar energy can be directly converted into electricity through photovoltaic effect. Being exposed to the sunlight, photons with energy greater than the band-gap energy of the semiconductor are absorbed and create some electron-hole pairs proportional to the incident irradiation. Under the influence of the internal electric fields of the p-n junction, these carriers are swept apart and create a photocurrent which is directly proportional to solar insolation that directly converts light energy into electricity.

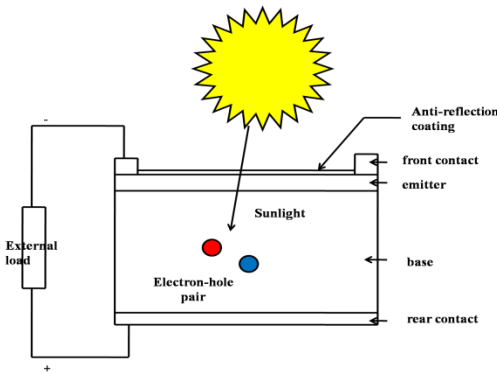


Fig.1.1 Basic structure for the operation of a PV cell

A solar cell is the building block of a solar panel. A photovoltaic module is formed by connecting many solar cells in series and parallel. Considering only a single solar cell; it can be modeled by utilizing a current source, a diode and two

resistors. This model is known as a single diode model of solar cell.

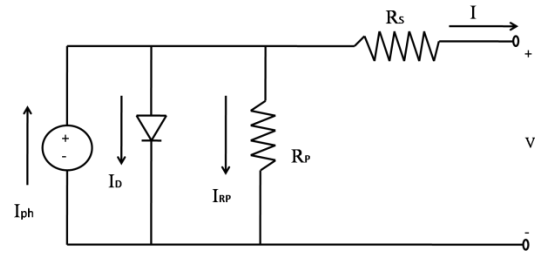


Fig.2.1 Single Diode Model of Solar Cell

Thus, this equation (4.1) represents that the output current generated depends on the PV module voltage, solar irradiance on PV module, wind speed, and ambient temperature

$$I = I_{ph} - I_{sat} \left[\exp \left\{ q * \frac{V + I * R_s}{A * k * T} \right\} - 1 \right] - \frac{V + I * R_s}{R_{sh}} \dots 2.1$$

where,

$$I_{sat} = I_{or} * \left(\frac{T}{T_r} \right)^3 * \left[\exp \left\{ q * E_{go} * \frac{1}{A * k} * \left(\frac{1}{T_r} - \frac{1}{T} \right) \right\} \right] \dots \dots \dots 2.2$$

$$I_{ph} = \{ I_{scr} + k_i * (T - 25) \} * \lambda \dots \dots \dots 2.3$$

• **Simplified single diode model**

Based on the single-diode model, the equivalent circuit is simplified by neglecting the shunt resistor. As a function of voltage, the current of a PV cell is given by

$$I = I_{ph} - I_d = I_{ph} - I_{sat} \left[\exp \left\{ \frac{V + I R_s}{V_t} \right\} \right] \dots \dots \dots 2.4$$

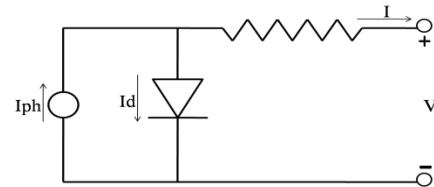


Fig.2.2 Open Circuit condition PV model

• **Open Circuit Condition**

One important points of the current-voltage characteristic must be pointed out: the open circuit voltage V_{oc} . At this points the power generated is also zero. When ever the current is zero, then only here will be the open circuit voltage i.e. $I=0$ and the shunt resistance R_{sh} is neglected.

$$V_{oc}(T) = V_{ocs} + \Delta V_{oc}(T - T_s) \dots \dots \dots 2.5$$

$$I_{sat}(G_a, T) = \frac{I_{ph}(G_a, T)}{e^{\left(\frac{V_{oc}(T)}{V_L(T)} \right) - 1}} \dots \dots \dots 2.6$$

$$V_{oc} \approx \frac{AKT}{q} \ln\left(\frac{I_L}{I_0} + 1\right) \dots\dots\dots 2.7$$

• Short Circuit Condition

In short circuit condition voltage is zero and current is maximum. .At this point power generated is zero. Equivalent circuit shown in Fig(3), the current relationship expressed as:

$$I_{ph} = I_d + I_{sc}$$

We know that the photo current I_{ph} is directly proportional to solar irradiance. Include the effect of irradiance and temperature on photo current, the photo current can be written as:

$$I_{ph}(G_a, T) = I_{scs} \frac{G_a}{G_{as}} [1 + \Delta I_{sc}(T - T_s)] \dots\dots\dots 2.8$$

• At the peak power point

The peak power point (V_{mpp} , I_{mpp}) under different testing environment can be known according to the photovoltaic panel's specification. At the peak power point,

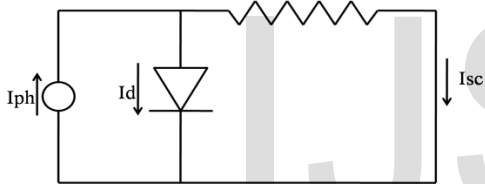


Fig.2.3 Short Circuit Condition PV Model

$$I_{mpp} = I_{ph} - \left[\frac{e^{\left(\frac{V_{mpp} + I_{mpp} R_s}{V_t}\right)} - 1}{e^{\left(\frac{V_{oc}}{V_t}\right)} - 1} \right] I_{ph} \dots\dots\dots 2.9$$

By re-organizing (2.9), we obtain the following relationship between R_s and V_s

$$R_s = \frac{V_t \ln \left[\left(1 - \frac{I_{mpp}}{I_{ph}} \right) e^{\left(\frac{V_{oc}}{V_t}\right)} + \frac{I_{mpp}}{I_{ph}} \right] - V_{mpp}}{I_{mpp}} \dots\dots\dots 10$$

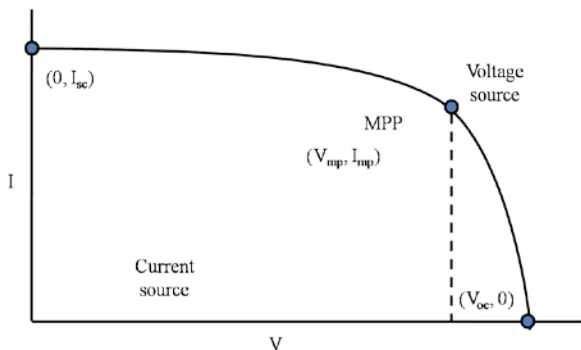


Fig.2.4 Characteristic I–V curve of a practical PV device and the three remarkable

points: short circuit ($0, I_{sc}$), MPP (V_{mp}, I_{mp}), and open circuit ($V_{oc}, 0$).

2.1 Maximum Power Point Tracking

The efficiency of a solar cell is very low. A typical solar panel converts only 30 to 40 percent of the incident solar irradiation into electrical energy. In order to increase the efficiency, methods are to be undertaken to match the source and load properly. One such method is the MPPT. This is a technique used to obtain the maximum possible power from a varying source. In photovoltaic systems the I-V curve

Is non-linear, thereby making it difficult to be used to power a certain load

Perturb and observe

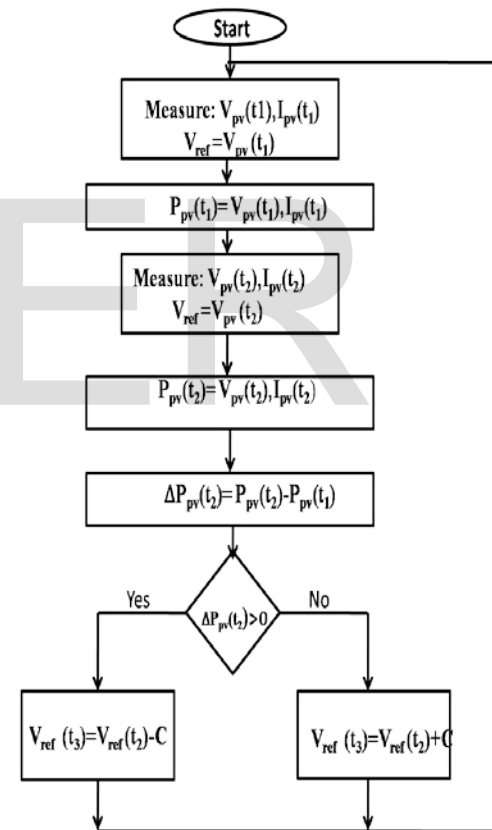


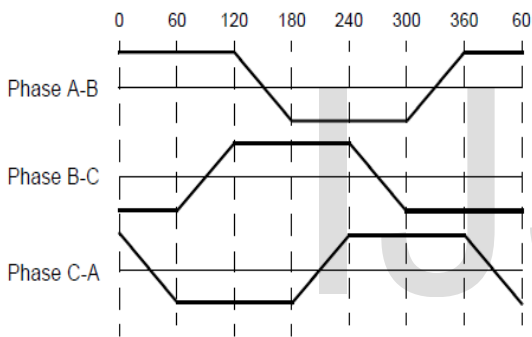
Fig.2.5 P&O method algorithm

3 BLDC Motor

A BLDC motor is considered to be a high performance motor that is capable of providing large amounts of torque over a vast speed range. BLDC motors are a derivative of the most commonly used DC motor, the brushed DC motor, and they

share the same torque and speed performance curve characteristics. The major difference between the two is the way these are having the arrangement of brushes. BLDC motors do not have brushes and must be electronically commutated, and hence it is called BLDC motor.

The back-emf is sinusoidal in case of PMSM, however in BLDC this back-emf is modified to trapezoidal, and due to this modification BLDC is said to be a modified form of PMSM. The “commutation region” of the back-emf of a BLDC motor should be as small as possible, while at the same time it should not be so narrow as to make it difficult to commutate a phase of that motor when driven by a Current Source Inverter. The flat constant portion of the back-emf should be 120° for a smooth torque production.



Trapezoidal Back Emf

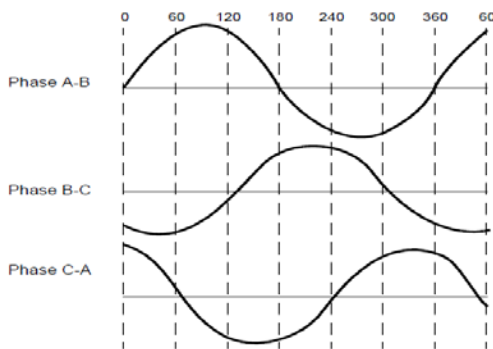


Fig 3.2 Sinusoidal Back Emf

3.1 BLDC drives operation with inverter

The BLDC is fed by a three-phase inverter as shown in fig. 3.3 and is basically an electronic motor. In self control mode the inverter acts like an electronic commutator that receives the

switching logical pulse from the absolute position sensors. The drive is also known as an electronic commutated motor.

Basically the inverter can operate in the following two modes.

- $2\pi/3$ angle switch-on mode
- Voltage and current control PWM model

- **$2\pi/3$ angle switch-on mode**

Inverter operation in this mode with the help of the wave from shown on Fig.3.6. The six switches of the inverter ($T_1 - T_6$) operate in such way so as to place the input dc current I_d symmetrical for $2\pi/3$ angle at the center of each phase voltage wave. The angle α shown is the advance angle of current wave with respect to voltage wave in the case α is zero. It can be seen that any instant, two switches are on, one in the upper group and another is lower group. For example instant t_1 , T_1 and T_6 are on when the supply voltage V_{dc} and current I_d are placed across the line ab (phase A and phase B in series) so that I_d is positive in phase a.

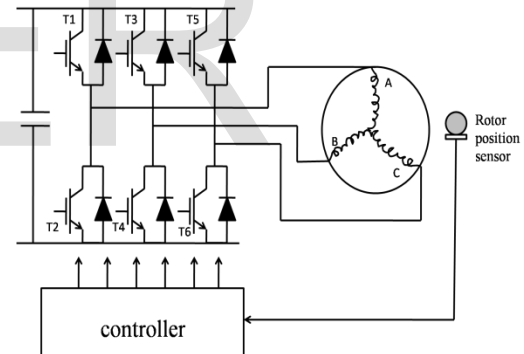


Fig 3.3 BLDC Motor Drive System

But negative in phase b then after $\pi/3$ interval (the middle of phase A). T_6 Is turned off and T_2 is turned on but T_1 continues conduction of the full $2\pi/3$ angle. This switching commutates $-I_d$ from phase b to phase c while phase a carry $+I_d$ the conduction pattern changes every $\pi/3$ angle indication switching modes in full cycle. The absolute position sensor dictates the switching or commutation of devices at the precise instants of wave. The inverter basically operating as a rotor position sensitive electronic commutator.

- **Voltage and current control PWM mode**

In the previous mode the inverter switches were controlled to give commutator function only when the devices were sequentially ON, OFF at $2\pi/3$ - angle duration .In addition to the commutator function, it is possible to control the switches in PWM chopping mode for controlling voltage and current continuously at the machine [3]terminal. There are essentially two chopping modes feedback (FB) mode and freewheeling mode. In both these modes devices are turned on and off on duty cycle basis to control the machine average current I_{AV} and the machine average voltage V_{AV} .

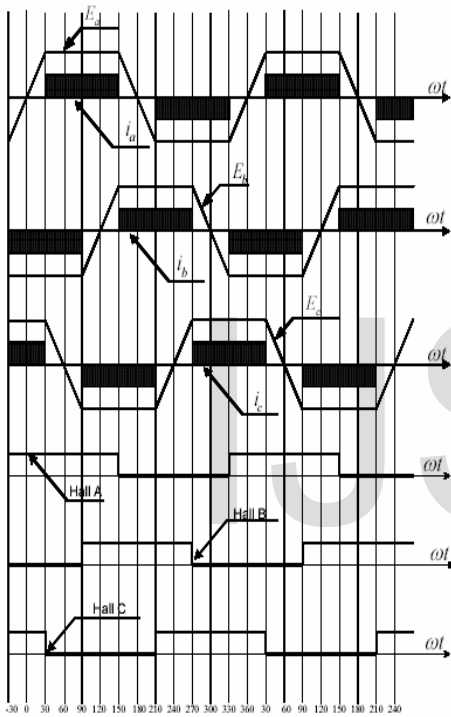


Fig 3.4 Back emfs, current waveforms and Hall Position Sensors for BLDC

3.2 Rotor position sensors

In order to produce a constant torque, the rotor position and the motor excitation are synchronized with the help of the necessary information provided by the Hall effect sensors. The change in magnetic field is detected by it. The rotor magnets are used as triggers the hall sensors. A signal conditioning circuit integrated with hall switch provides a TTL-compatible pulse with sharp edges. Three hall sensors are placed 120 degree apart are mounted on the stator frame. The hall sensors digital signals are used to sense the rotor position.

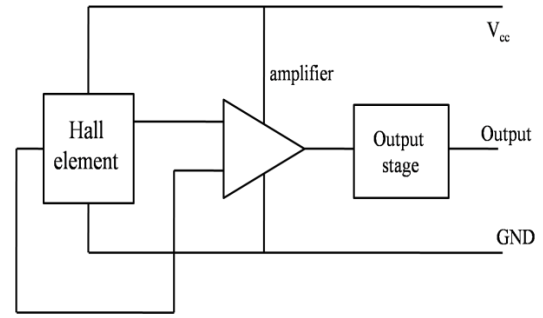


Fig 3.5 Hall position sensors

3.3 Mathematical Model of BLDC Motor

The BLDC motor consists of three stator windings and permanent magnets on the rotor. Since both the magnet and the stainless steel retaining sleeves have high resistivity, rotor-induced currents can be neglected and no damper windings are modeled. Hence the circuit equations of the three windings in phase variable are

$$\begin{bmatrix} v_a \\ v_b \\ v_c \end{bmatrix} = \begin{bmatrix} R & 0 & 0 \\ 0 & R & 0 \\ 0 & 0 & R \end{bmatrix} \begin{bmatrix} i_a \\ i_b \\ i_c \end{bmatrix} + p \begin{bmatrix} L_{aa} & L_{ba} & L_{ca} \\ L_{ba} & L_{bb} & L_{cb} \\ L_{ca} & L_{cb} & L_{cc} \end{bmatrix} \begin{bmatrix} i_a \\ i_b \\ i_c \end{bmatrix} + \begin{bmatrix} e_a \\ e_b \\ e_c \end{bmatrix} \dots\dots\dots 3.1$$

where v_a , v_b and v_c are the stator phase voltages; R is the stator resistance per phase; i_a , i_b and i_c are the stator phase currents; L_{aa} , L_{bb} and L_{cc} are the self-inductance of phases a, b and c; L_{ab} , L_{bc} and L_{ac} are the mutual inductances between phases[6] a, b and c; the phase back electromotive forces are e_a , e_b and e_c . It has been assumed that resistance of all the winding are equal. It also has been assumed that if there in no change in the rotor reluctance with angle because of a no salient rotor and then

$$L_{aa} = L_{bb} = L_{cc} = L$$

$$L_{ab} = L_{ba} = L_{ac} = L_{ca} = L_{bc} = L_{cb} = M$$

Hence

$$\begin{bmatrix} v_a \\ v_b \\ v_c \end{bmatrix} = \begin{bmatrix} R & 0 & 0 \\ 0 & R & 0 \\ 0 & 0 & R \end{bmatrix} \begin{bmatrix} i_a \\ i_b \\ i_c \end{bmatrix} + p \begin{bmatrix} L & M & M \\ M & L & M \\ M & M & L \end{bmatrix} \begin{bmatrix} i_a \\ i_b \\ i_c \end{bmatrix} + \begin{bmatrix} e_a \\ e_b \\ e_c \end{bmatrix} \dots\dots\dots 3.2$$

The stator phase currents are constrained to be balanced i.e.

$$i_a + i_b + i_c = 0 \dots\dots\dots 3.3$$

This leads to the simplifications of the inductances matrix in the models as then

$$Mi_b + Mi_c = -Mi_a \dots\dots\dots 3.4$$

Hence

$$\begin{bmatrix} v_a \\ v_b \\ v_c \end{bmatrix} = \begin{bmatrix} R & 0 & 0 \\ 0 & R & 0 \\ 0 & 0 & R \end{bmatrix} \begin{bmatrix} i_a \\ i_b \\ i_c \end{bmatrix} + p \begin{bmatrix} L-M & 0 & 0 \\ 0 & L-M & 0 \\ 0 & 0 & L-M \end{bmatrix} \begin{bmatrix} i_a \\ i_b \\ i_c \end{bmatrix} + \begin{bmatrix} e_a \\ e_b \\ e_c \end{bmatrix} \dots\dots\dots 3.5$$

It has been assume that back EMF e_a , e_b and e_c are have trapezoidal wave from

$$\begin{bmatrix} e_a \\ e_b \\ e_c \end{bmatrix} = \omega_m \lambda_m \begin{bmatrix} f_{as}(\theta_r) \\ f_{bs}(\theta_r) \\ f_{cs}(\theta_r) \end{bmatrix} \dots\dots\dots 3.6$$

where ω_m the angular rotor speed in radians per seconds, λ_m is the flux linkage, θ_r is the rotor position in radian and the functions $f_{as}(\theta_r)$, $f_{bs}(\theta_r)$, and $f_{cs}(\theta_r)$ have the same shape as e_a , e_b and e_c with a maximum magnitude of ± 1 . The induced emfs do not have sharp corners because these are in trapezoidal nature.

The emfs are the result of the flux linkages derivatives and the flux linkages are continuous function. Fringing also makes the flux density function smooth with no abrupt edges.

The electromagnetic torque in Newton's defined as

$$T = [e_a i_a + e_b i_b + e_c i_c] / \omega_m \quad (\text{Nm}) \dots\dots\dots 3.7$$

It is significant to observe that the phase voltage-equation is identical to armature voltage equation of dc machine. That is one of reasons for naming this machine the PM brushless dc machine.

The potential of the neutral point with respect to the zero potential (v_{n0}) is required to be considered in order to avoid imbalance in the applied voltage and simulate the performance of the drive. This is obtained by substituting equation (3.3) in the volt-ampere equation (3.5) and adding then give as

$$v_{a0} + v_{b0} + v_{c0} - 3v_{n0} = R_s(i_a + i_b + i_c) + (L - M)(pi_a + pi_b + pi_c) + (e_a + e_b + e_c) \dots\dots\dots 3.8$$

Substituting equation (3.3) in equation (3.8) we get

$$v_{a0} + v_{b0} + v_{c0} - 3v_{n0} = (e_a + e_b + e_c) \dots\dots 3.9$$

thus

The set of differential equations mentioned in equations (3.5), and (3.10). Defines the developed model in terms of the variables i_a , i_b , i_c , ω_m and, θ_r time as an independent variable.

$$v_{n0} = v_{a0} + v_{b0} + v_{c0} - (e_a + e_b + e_c) / 3 \dots\dots\dots 3.10$$

Combining the all relevant equations, the system in state-space form is

$$x = Ax + Bu + Ce \dots\dots\dots 3.11$$

where

$$x = [i_a \ i_b \ i_c \ \omega_m \ \theta_r]^t \dots\dots\dots 3.12$$

$$A = \begin{bmatrix} -\frac{R_s}{L-M} & 0 & 0 & \frac{\lambda_m}{J} f_{as}(\theta_r) & 0 \\ 0 & -\frac{R_s}{L-M} & 0 & \frac{\lambda_m}{J} f_{bs}(\theta_r) & 0 \\ 0 & 0 & -\frac{R_s}{L-M} & \frac{\lambda_m}{J} f_{cs}(\theta_r) & 0 \\ \frac{\lambda_m}{J} f_{as}(\theta_r) & \frac{\lambda_m}{J} f_{bs}(\theta_r) & \frac{\lambda_m}{J} f_{cs}(\theta_r) & -\frac{B}{J} & 0 \\ 0 & 0 & 0 & \frac{P}{2} & 0 \end{bmatrix} \dots\dots\dots 3.13$$

$$B = \begin{bmatrix} \frac{1}{L-M} & 0 & 0 & 0 \\ 0 & \frac{1}{L-M} & 0 & 0 \\ 0 & 0 & \frac{1}{L-M} & 0 \\ 0 & 0 & 0 & \frac{1}{L-M} \end{bmatrix} \dots\dots\dots 3.14$$

$$C = \begin{bmatrix} -\frac{1}{L-M} & 0 & 0 \\ 0 & -\frac{1}{L-M} & 0 \\ 0 & 0 & -\frac{1}{L-M} \end{bmatrix} \dots\dots\dots 3.15$$

4 SIMULATION AND RESULTS

Simulink Model of Solar Cell with BLDC Motor

The Simulink model of the PV system used for the implementation in driving the BLDC motor, alongwith the boost converter and inverter is shown in fig 4.

In this Simulation model, a PV array is chosen and given the variable irradiance in terms of constant, step and ramp inputs. The maximum power of this PV array is taken using the MPPT which is developed using the P & O algorithm.

The various other elements which are used to construct this model include the boost converter, which is used to step up the voltage to the required value. The IGBT based inverter is used to convert the dc voltage into the ac voltage and the input to this inverter is provided using the PWM generator, in which the signals are generating from the control circuit. The inverter is then connected to the L-C filter to eliminate the harmonics of the ac voltage. This voltage is therefore needed for driving a three-phase parallel RLC load attached to the system, and basically to provide the sufficient voltage to drive the BLDC motor load.

Power system block in the MATLAB. The simulation model is as shown.

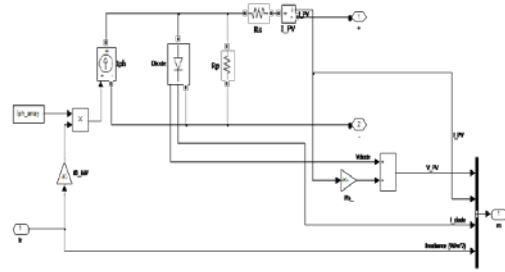


Fig. 4.1 Simulation model of a PV Array

A controlled current source is been used to drive the solar cell. The PV array is then constructed using various number of solar cells connected in series and in parallel. The input to this array is provided for different solar irradiancies.

Solar Cell with MPPT

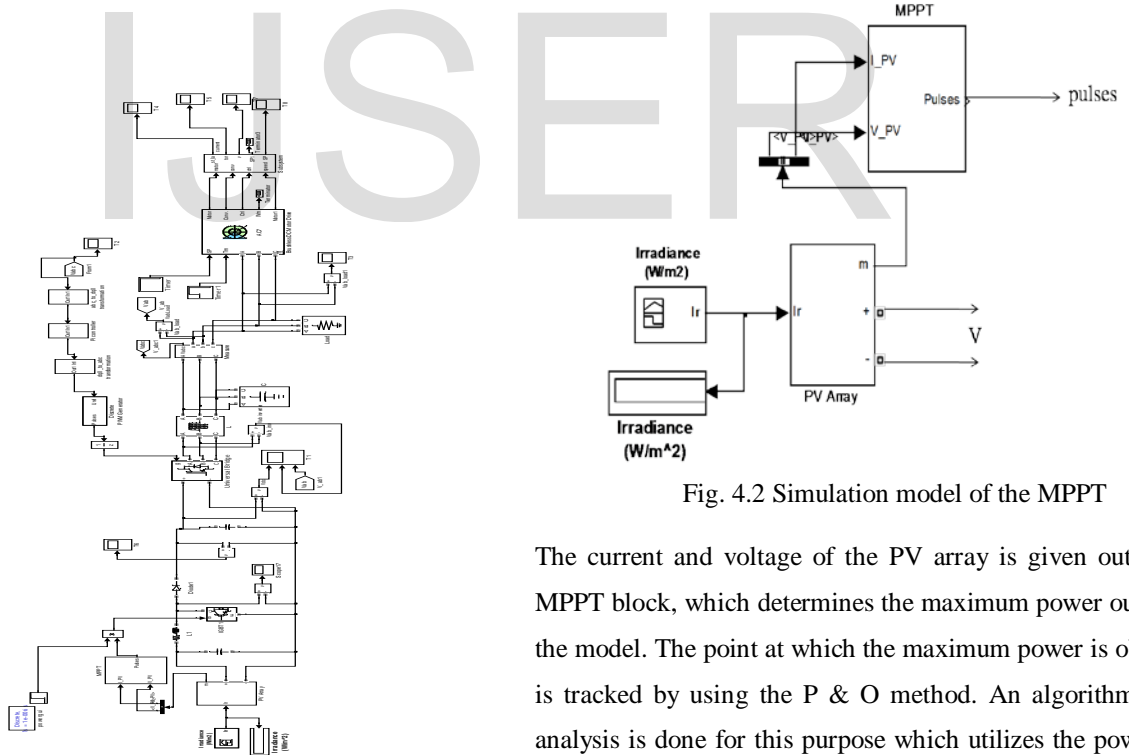


Fig. 4.2 Simulation model of the MPPT

The current and voltage of the PV array is given out to the MPPT block, which determines the maximum power output of the model. The point at which the maximum power is obtained is tracked by using the P & O method. An algorithm based analysis is done for this purpose which utilizes the power and voltage values being measured at different time intervals and a comparison based study is carried out to locate the MPP.

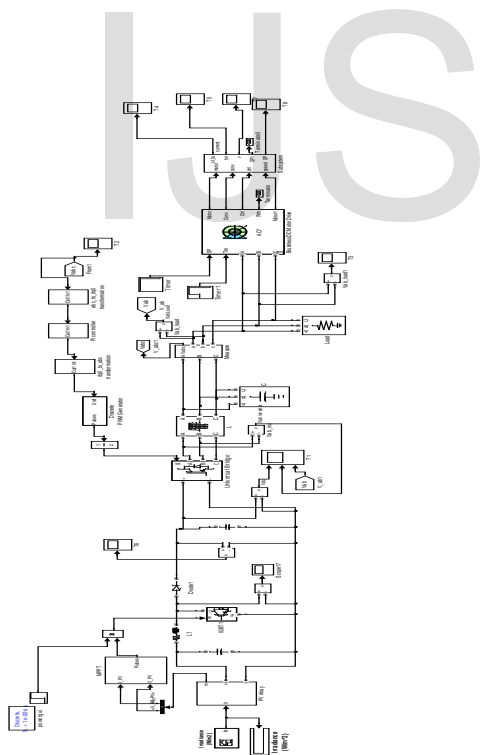


Fig 4 simulation Model of the whole System

Single Diode PV Model

The PV cell is constructed using the single diode model. The I_{ph} which is given in the input of the cell model is basically the photo-generated current. This consists of a R_s resistor in series and R_p resistor in parallel. This was modeled using the Sim

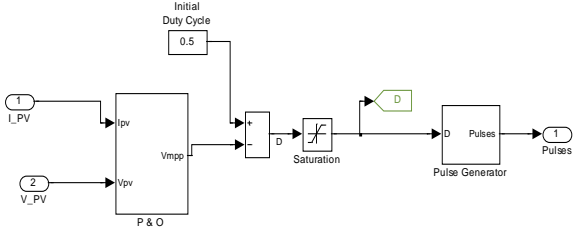


Fig 4.3 Modeling of P&O Algorithm

The unit in which the gating signal is provided uses the MPPT algorithm of the P & O method where the change in power, change in voltage, instantaneous power and instantaneous current values are taken into account to do the necessary duty cycle variations. The repeating sequence being utilized in the model has an operating frequency of f KHz. This is also the frequency of the gating signal.

DC-DC Converter Circuit

The dc-dc boost converter is utilized to step up the voltage to the specified level and it consists of a L mH inductor with a R ohm resistor and a C μ F capacitor. The gating signal to the boost converter is generated by comparing the signal generated by the MPPT algorithm to a repeating sequence operating at a high frequency

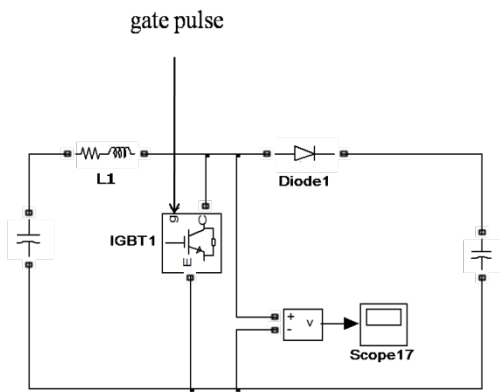


Fig 4.4 DC-DC Boost Converter

Inverter Circuit

The dc voltage which is coming from the dc-dc converter is converted to the ac voltage using the IGBT based inverter, which is modeled using the blocks provided in the library icon

of MATLAB. The gating signal to this inverter is provided from the control circuitry which is explained later.

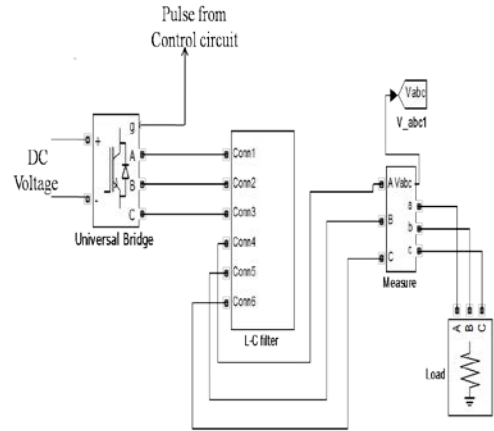


Fig. 4.5 Simulation Model of the Inverter Circuit

Control Circuit

The three-phase ac voltage which is obtained after the overall simulation and measured by the three-phase measurement block of the simulink library is given in the input of the three-phase PLL block, which tracks the frequency and phase of a sinusoidal three-phase signal by using an internal frequency oscillator, which helps to keep the phase difference to zero. The three-phase sinusoidal voltage obtained from the PLL block is then applied to the abc to dq0 transformation block, which computes the direct axis, quadratic axis, and zero sequence quantities in a two-axis rotating reference frame for a three-phase sinusoidal signal. The two-axis transformed voltage is compared with the reference values of the direct axis and quadrature axis and through the selector are given to the PI controller block, which uses the gains to tune the response time, overshoot, and steady-state error performances. The voltage from this block is further applied to the inverse Park transformation block, which change the two-axis rotating reference frame voltages back to the three-phase voltages. These voltages are then given to the PWM pulse generator having a carrier frequency of F_C KHz, and the signals provided from this generator are applied to the inverter.

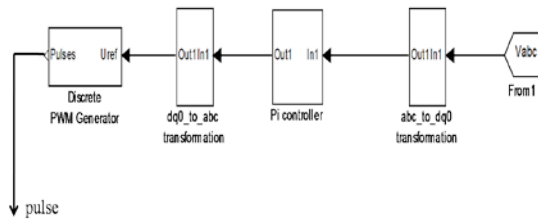


Fig. 4.6 Simulation model of the Control circuit

BLDC Motor Drive

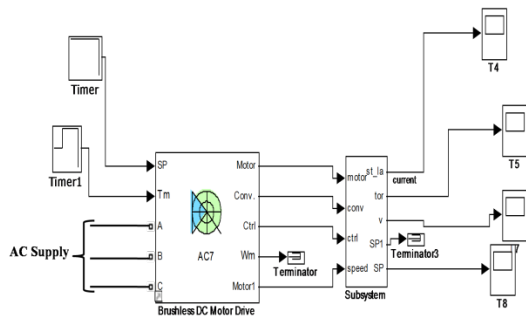


Fig. 5.8 Simulation Model of BLDC Motor

A permanent magnet BLDC motor with the mechanical input as the torque is taken from Sim Power Systems library in the Matlab software. It consists of a speed controller, the braking chopper, and the current controller and these models are specific to the Electric Drives library. The torque and speed set time is controlled by a timer and similarly a timer is set for the torque, which is the input to the motor. The various parameters of the BLDC motor, such as the stator current, electromagnetic torque are then analyzed using the whole PV system model. Moreover, speed control of motor is also provided.

Results

The PV module consists of following parameters:

Number of cells per module = 96

Number of series-connected modules per string = 5

Number of parallel strings = 66.

Irradiance = 1000 W/m²

The dc voltage which is generated by the PV array is of very low magnitude of 300 V and after boosting it through the dc-dc converter it reaches to a much greater amplitude, i.e. up to 480 V, shown in figure 5.1. The dc voltage after attaining the higher magnitude level while passing it through the boost converter is converted to the ac voltage, shown in figure 5.2 and the harmonics of this voltage are eliminated with the help of L-C filter. After, filtering the load voltage is obtained as shown in figure 5.3.

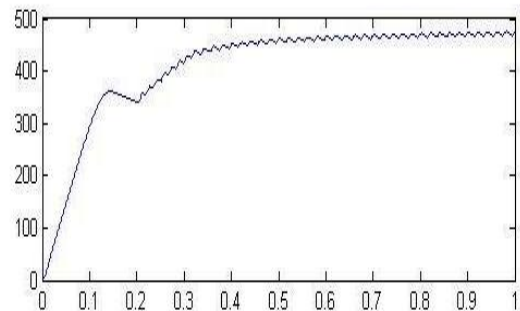


Fig.5.1 DC Voltage

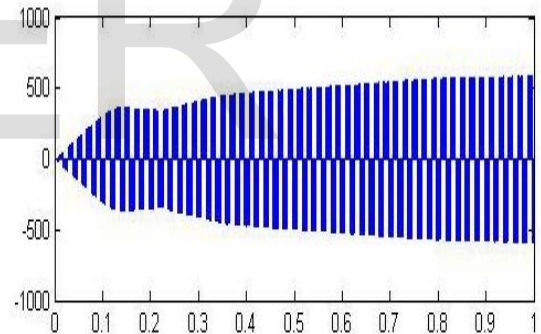


Fig.5.2 Inverter Voltage

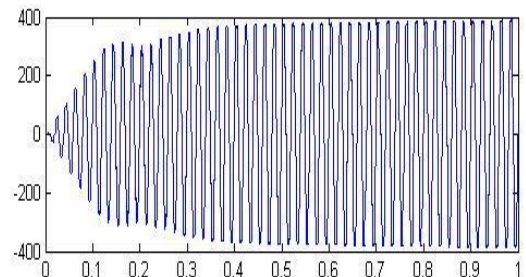


Fig.5.3 Load Voltage

Motor Results

The BLDC motor used has the following parameters:

Parameters	Value
Supply Voltage	380 V
Frerquency	50 Hz
Number of Poles	4
Motor Rating	2.2 kW (3 HP)
Nominal Speed	1650 rpm

Table 5.1 Parameters chosen for the simulation

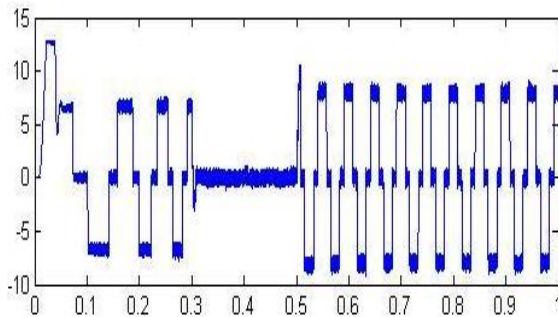


Fig.5.4 Stator Current

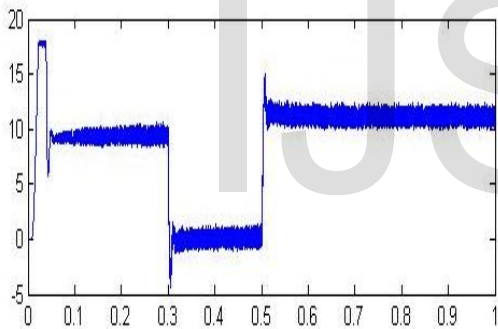


Fig.5.5 Load Torque

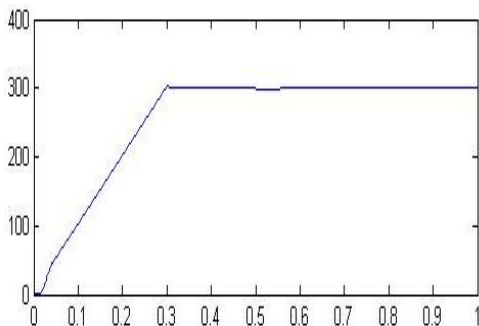


Fig.5.6 Speed of the Motor

(1)The speed is maintained at the set point value of 300 rpm, at time $t=0$ seconds. After observing, it is concluded that the speed follows the acceleration ramp precisely.

(2)At time $t=0.5$ seconds, the full load torque is applied to the motor. On observing, a small disturbance in the motor speed, which stabilizes very quickly.

(3)At time $t=1$ second, the speed set point is changed to 0 rpm. The speed decreases to zero rpm following the deceleration ramp precisely.

FFT ANALYSIS

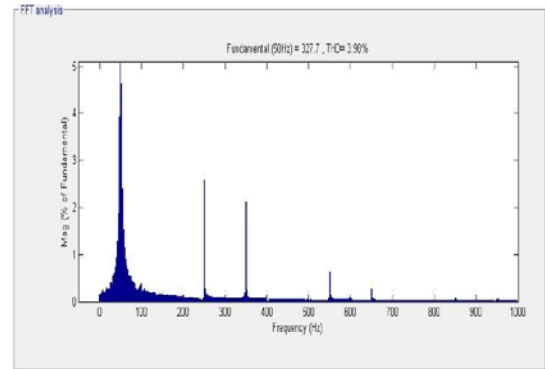


Fig 5.7 FFT Analysis of Load Voltage

The FFT analysis of the line voltage is shown in figure 5.7 and total harmonic distortion (THD) gets reduce to 3.98%, and hence the lower order harmonics are eliminated.

5 CONCLUSION

The thesis provides the working of the brush-less direct current motor having certain specifications and the motor operated efficiently and the results of the parameter variations were plotted and designed as per the simulation work. The dissertation provides a basic idea for the economical and efficient use of the solar energy to drive the industrial motor and to operate these motors depicting their characteristic features so that an analysis based study could be carried out to determine their overall progress while in operation.

The use of renewable energy as a source help us to ensure effective and efficient working of the motor, since now-a-days the BLDC motor is used in several industrial and medical applications. The thesis provides the development of the MPPT method which provided the use of such a higher rating motor with ease and with the successful operation of the motor.

ACKNOWLEDGEMENT

First of all, I would like to Thank my Parents for providing me support and resources, which helped me to complete my paper successfully and also for supporting my interest in this field. Next, I would like to express heartily gratitude to my supervisor, Prof. (Dr.) P.B.L. Chaurasia, Dean Engineering & Director, Centre of Excellence, Solar Energy Research & Utilization for his valuable technical suggestions and full guidance towards completion of my paper from the beginning till the end.

REFERENCES

- [1] Mairaj Aftab Malik, Omar Kiyani, and Arvind Srinivasan, "Alternative Solar Cells and Their Implications", An Interactive Qualifying Project, Worcester Polytechnic Institute, MA, March 2010.
- [2] Weidong Xiao, William G. Dunford, and Antoine Capel, "A Novel Modeling Method for Photovoltaic Cells", 35th Annual IEEE Power Electronics Specialists Conference, Germany, pp. 1950-1956, 2004.
- [3] M. G. Villalva, J. R. Gazoli, and E. R. Filho, "Comprehensive Approach to Modeling and Simulation of Photovoltaic Arrays", IEEE Trans. Power Electronics, Vol. 24, No.5, pp. 1198-1208, May 2009.
- [4] M. Berrera, A. Dolara, R. Faranda and S. Leva, "Experimental test of seven widely-adopted MPPT algorithms", 2009 IEEE Bucharest Power Tech Conference, June 28th - July 2nd, Bucharest, Romania.
- [5] "Modeling simulation and analysis of a permanent magnet brushless dc motor drive," presented at the IEEE IAS Annual Meeting, Atlanta, 1987.
- [6] S. Funabiki and T. Himei, "Estimation of torque pulsation due to the behavior of a converter and an inverter in a brushless dc-drive system," Proc. Inst. Elec. Eng., vol. 132, part B, no. 4, pp. 215-222, July 1985.
- [7] P. Pillay and R. Krishnan, "Modeling, Simulation and Analysis of a Permanent Magnet Brushless DC motor drive part II: The brushless DC motor drive," IEEE Transactions on Industry application, Vol.25, May/Apr 1989.
- [8] S. Rambabu, "Modeling and Control of a Brushless DC Motor", A Thesis for the degree of Master of Technology, National Institute of Technology, Rourkela, 2007.
- [9] A. Tashakori, M. Ektesabi, N. Hosseinzadeh, "Modeling of BLDC Motor with Ideal Back-EMF for Automotive Applications", Proceedings of the World Congress on Engineering 2011 Vol II WCE 2011, July 6 - 8, 2011, London, U.K.
- [10] Vinod Kr Singh Patel, A.K. Pandey, "Modeling and Simulation of Brushless DC Motor Using PWM Control Technique", IJERA, Vol. 3, Issue 3, May-Jun 2013, pp.612-620.
- [11] Pierre Voultoury, "Sensorless Speed Controlled Brushless DC Drive using the TMS320C242 DSP Controller", Application Report SPRA498, Digital Signal Processing Solutions, Texas Instruments.
- [12] Atmel AVR443: Sensor-based Control of Three Phase Brushless DC Motor [Application Note] 2596C-AVR-07/2013.
- [13] Y. Zhang and J. Zhu, "Direct torque control of permanent magnet synchronous motor with reduced torque ripple and commutation frequency," IEEE Trans. Power Electron., vol. 26, no. 1, pp. 235-248, Jan. 2011.
- [14] Ronald De Four, Emily Ramoutar and Juliet Romeo, "Operational Characteristics of Brushless DC Motors", The University of the West Indies St. Augustine, Trinidad.
- [15] Preetha Philip, Dr. Meenakshy, "Modelling Of Brushless DC Motor Drive Using Sensored and Sensorless Control (back EMF zero crossing detection)", IJEATE, Volume 2, Issue 8, August 2012.
- [16] Ms. Juli Singh, "Analysis The Speed Control of BLDC Motor Drive Using Sensors", IJERA, Vol. 2, Issue 3, May-Jun 2012, pp.2868-2884.
- [17] S. Satpathy, "Photovoltaic Power Control Using MPPT And Boost Converter", A Thesis submitted for the degree of Master of Technology, National Institute of Technology, Rourkela, May 2012.

IJSER